

Curriculum reinforcement learning for tokamak control

Abstract

1 Tokamaks are the leading candidates to achieve nuclear fusion as a sustainable source of energy, and plasma control plays a crucial role in their operations. However, the complex behavior of plasma dynamics makes control of these devices challenging through traditional methods. Recent works proved the usefulness of reinforcement learning as an efficient alternative, in order to fulfill these high-dimensional and non-linear situations. Despite their performance, controlling relevant plasma configurations requires expensive and long training sessions on simulations. In this work, we leverage the use of a curriculum strategy to achieve significant speed-up in learning a controller for the control coils, which tracks plasma quantities such as shape, position and current. To this end, we developed a fast, asynchronous and reliable framework to enable interactions between a distributed actor-critic and a C++ code simulating the WEST tokamak. By sequentially increasing task complexity, results show a clear reduction in convergence time and training cost. This work is one of the first attempts to enable fast production of robust magnetic controllers, for routine use in the operations of a magnetically confined fusion device.

1 Introduction

27 Mastering nuclear fusion could significantly impact the world, unlocking the path towards sustainable and attractive means of energy production. With no direct high-level byproducts of the reaction, it has many advantages over conventional energy sources [Ariola and Pironti, 2008]. To harness this potential alternative, tokamaks are promising devices to maintain the stability and performance of plasma's confinement, despite numerous physical and control challenges [Meade, 2009].

36 Tokamaks are torus-shaped devices which aim at sustaining fusion reactions within a plasma under specific temperature and density conditions [Wesson, 2004]. They rely on magnetic fields generated by both *toroidal* and *poloidal* field coils (PFC) to shape it. Interactions occur at different levels with complex dynamics involved between the plasma and its

surroundings. Control systems are then required to adjust the voltages applied to the PFCs (Figure 2), allowing control of quantities intrinsically linked to plasma's evolution, like position of the magnetic center m , *Last Closed Flux Surface* (LCFS), elongation κ and current I_p (Figure 1). To study the effects of various plasma configurations, scientists rely on real-time linear controllers [Nouailletas and et al., 2023], which require substantial engineering effort whenever target scenarios undergo variations. Hence, there is an essential need for flexibility, adaptability and robustness of magnetic control systems through the entirety of the device lifetime, without which no sustained plasma could be produced.

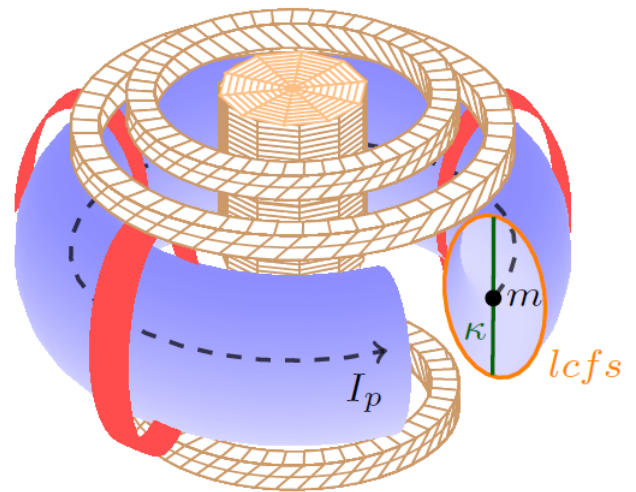


Figure 1: Control quantities of interest with toroidal (red) and poloidal (strided gold) sections.

Reinforcement Learning (RL) [Sutton and Barto, 2018] emerged as an innovative approach to numerous real-time control problems. Despite impressive results in a variety of domains [Han *et al.*, 2023; Brohan and et al., 2023; Kiran and et al., 2022], it usually relies on either fast and precise simulation enabling the collection of vast amount of experiences, or on direct sampling from a physical device. Both cases can not be fulfilled in our context: sampling of experimental data on the plant for the sole purpose of training is impractical, and simulations remain expensive in order to ac-

64 count for the coupled behavior of plasma dynamics. Despite
 65 the existence of distributed architectures as powerful tools to
 66 compensate for these bottlenecks, training still remains long
 67 and costly as the number of parallel environments increases.

68 In this work, we study the effects of a curriculum strategy
 69 on learning a magnetic controller through a distributed rein-
 70 forcement learning framework. By improving training speed
 71 and performance, we intend to accelerate the production
 72 of robust magnetic controllers for the operation of WEST,
 73 a supraconductive tokamak located at CEA Cadarache¹ in
 74 Saint-Paul-lez-Durance, France [Bourdelle and et al., 2015;
 75 Bucalossi and et al., 2022]. Indeed, such methodology could
 76 assist plasma researchers in quickly obtaining controllers, or
 77 adapt existing ones, for each new experimental campaign,
 78 hence improving flexibility and adaptability of RL-based
 79 magnetic control.

80 Next sections will be organized as follows. First, we will
 81 give an overview of the related work regarding RL for toka-
 82 maks, and curriculum strategies in RL. We will then describe
 83 the curriculum methodology within plasma magnetic control,
 84 and the overall training framework. Finally, experiments are
 85 discussed through validation and analysis of the learned poli-
 86 cy. The latter will be compared to a baseline agent obtained
 87 without the strategies of interest. Finally, we will conclude
 88 on this study and its perspectives.

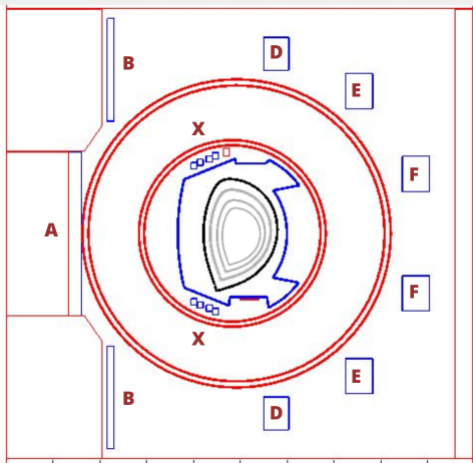


Figure 2: Cross-section with surrounding control coils, namely poloidal field coils.

89 2 Background

90 2.1 Reinforcement learning for tokamaks

91 A classical RL framework sets an agent which interacts
 92 with an environment formalized as a *Markov Decision Pro-*
 93 *cess (MDP)* denoted \mathcal{M} . This MDP is defined by a state
 94 space \mathcal{S} , an action space \mathcal{A} , its state transition distribution
 95 $P(s'|s, a) : \mathcal{S} \times \mathcal{A} \times \mathcal{S} \rightarrow [0, 1]$, an initial state distribution
 96 $P^0(s) : \mathcal{S} \rightarrow [0, 1]$, and a reward signal $R(s, a) : \mathcal{S} \times \mathcal{A} \rightarrow \mathbb{R}$.

97 Starting from state $s_0 \sim P^0(\cdot)$, the agent must learn an
 98 optimal policy $\pi^* : \mathcal{S} \times \mathcal{A} \rightarrow [0, 1]$, which maximizes the

discounted cumulative reward, or *return*, over the course of
 an episode, i.e a trajectory over states and actions from the
 interactions with the environment:

$$\pi^* = \operatorname{argmax}_{\pi_{\theta}} \mathbb{E}_{(s_0, a_0, \dots, s_t, a_t)} \left[\sum_{k=0}^{\infty} \gamma^k r_{t+k} \right] \quad (1)$$

with discount factor $\gamma \in [0, 1]$ working as a penalization
 term for long-term rewards, and $r_t = R(s, a) = \mathbb{E}[r_{t+1} | s_t =$
 $s, a_t = a]$. Most importantly, the reward function is a scalar
 feedback signal which indicates how well the agent performs
 with respect to the overall objectives, hence the importance
 of its design. The feedback loop between the agent and the
 environment ends once a terminal condition is reached, like
 a situation that we want to avoid, or a threshold on simulated
 time. As a side note, the policy can be deterministic, assign-
 ing a probability of 1 to the same action for each observed
 state. Moreover, it can be a parametrized function, like a neu-
 ral network. In such cases, it is usually denoted by π_{θ} , where
 θ are the weights of the said model.

Fundamental definitions arise with the value function
 $V_{\pi_{\theta}}(s) = \mathbb{E}_{\pi_{\theta}} [\sum_{k=0}^{\infty} \gamma^k r_{t+k} | s_t = s]$, and the action-value
 function $Q_{\pi_{\theta}}(s, a) = \mathbb{E}_{\pi_{\theta}} [\sum_{k=0}^{\infty} \gamma^k r_{t+k} | s_t = s, a_t = a]$.
 It is worth mentioning that relying on the first is difficult
 in real-world applications such as fusion, since they do not
 exhibit proper knowledge of the probability transition func-
 tion P . Because of that, making actions explicit is an inter-
 esting way of computing the expected return, as state-
 action pairs can be easily sampled throughout learning. Over
 the past years, the use of neural networks (NN) as power-
 ful action-value and policy approximators lead to major ad-
 vancements in continuous control problems. Deep RL algo-
 rithms such as ones from the actor-critic family kept increas-
 ing in efficiency, leading to precise control in several high-
 dimensional and non-linear control problems [Grondman *et*
al., 2012], both in on-policy [Schulman and et al., 2015;
 Schulman and et al., 2017; Mnih and et al., 2016] and off-
 policy settings [Haarnoja *et al.*, 2018; Fujimoto *et al.*, 2018;
 Lillicrap and et al., 2015].

Consequently, deep reinforcement learning is becoming in-
 creasingly popular among the plasma control community. For
 example, RL has been used for model-based control [Char
 and et al., 2023], for vertical stabilization [Dubbioso *et al.*,
 2023; De Tommasi *et al.*, 2022], to build feedforward tra-
 jectories of plasma parameters [Seo and et al., 2021], for
 temperature and profile control [Wakatsuki and et al., 2019;
 Wakatsuki *et al.*, 2021], or even for tearing instability control
 and disruption avoidance [Seo *et al.*, 2024]. Recent works
 [Degraeve and et al., 2022] designed a RL-based system which
 achieved magnetic control of the *Tokamak à Configuration*
Variable (TCV), in Lausanne, Switzerland. The learned con-
 troller demonstrates the capability for RL-based systems to
 tackle various complex plasma configurations while tracking
 many quantities of interest at the same time. A similar proce-
 dure was proposed by [Kerboua-Benlarbi *et al.*, 2024], with
 the same limitations of the initial proposal, while refining the
 simulation on which magnetic controllers were trained.

These examples highlight a shift of focus from classical
 controllers, designed using prior knowledge on how control

¹French Alternative Energies and Atomic Energy Commission

154 should be performed with respect to physical properties of the
155 dynamical system, to controllers learning by trial-and-error
156 to act on the system based on what should be achieved in
157 terms of final objectives. In summary, deep RL advantages
158 over classical tokamak control stem from its ability to: ful-
159 fil these high dimensional, uncertain and non-linear systems;
160 explore possible strategies in order to make the control policy
161 more flexible in contrast with the fixed heuristics of classical
162 control; learn from raw magnetic signals using neural net-
163 works, since plasma quantities can not be measured directly,
164 and are instead usually inferred in real-time from reconstruc-
165 tion codes [Faugeras, 2020; Carpanese, 2021] for use by clas-
166 sical controllers.

167 2.2 Curriculum learning for reinforcement 168 learning

169 Curriculum learning (CL) [Bengio *et al.*, 2009] is a method-
170 ology to optimize the order in which experiences are pro-
171 cessed by an agent over the course of training. From the
172 early stages of human development to adulthood, learning is
173 structured and organized sequentially, so that the knowledge
174 acquired over time facilitates the understanding of new no-
175 tions or tasks that occur later to us. Therefore, a sequence
176 of increasingly difficult tasks implicitly builds a curriculum,
177 as knowledge is transferred from one intermediate objective
178 to the other. Scheduling and designing such strategy helps in
179 acquiring transferable skills to guide exploration during train-
180 ing, with the premise of increasing performance and reduce
181 convergence time towards a final set of tasks.

182 Recent works classified the taxonomy of existing methods
183 [Soviany *et al.*, 2022] as well a mathematical framework for
184 curriculum learning in reinforcement learning domains using
185 graphs [Narvekar *et al.*, 2020]. In most cases, we consider
186 different MDPs between each task and three main concepts
187 arise with which CL methods can be classified: the interme-
188 diate task generation, the partial ordering on the obtained set
189 of tasks and how knowledge could be shared between its ele-
190 ments. Considering the importance of human intuition to de-
191 fine simple tasks [Bengio *et al.*, 2009], domain experts could
192 efficiently make a distinction between objectives that are nei-
193 ther "too easy" or "too hard". Indeed, task generation and se-
194 quencing of the latter could be handcrafted from human op-
195 erators [MacAlpine and Stone, 2018; Stanley *et al.*, 2005],
196 but both concepts could be built up automatically as part
197 of the curriculum learning procedure [Graves *et al.*, 2017;
198 Wu and Tian, 2017; Ivanovic and *et al.*, 2019]. Transfer learn-
199 ing methods are required to share knowledge representation
200 at each step of the curriculum, and concern several elements
201 of the training loop, such as entire policies and value func-
202 tions, rewards, etc [Zhu *et al.*, 2023]. Care must be taken
203 while choosing the right combinations of methods, to avoid
204 negative transfer which could harm controllers performance
205 [Wolczyk *et al.*, 2022].

206 3 Approach

207 3.1 Motivation

208 RL is still an emerging field within plasma magnetic con-
209 trol, and few applications are observable. It can take sev-

210 eral days of training for efficiency on relative simple plasma
211 scenarios [Degrave and *et al.*, 2022; Kerboua-Benlarbi *et al.*,
212 2024]. Nevertheless, the routine operation of a tokamak re-
213 quires flexibility over the design of controllers. Minimum
214 engineering efforts should be targeted to adapt and fine-tune
215 the controllers with respect to the objectives of each new ex-
216 perimental campaign.

217 For this reason, this study aims at assessing the effects of
218 CL in the context of fusion, where poor reward signal and
219 state representation at the beginning of learning, can desta-
220 bilize the whole training process. We do not specifically in-
221 tend to reach a new general performance threshold, but look
222 for increased performance at start of each new task, special-
223 izing exploration as training evolves towards its final goal.
224 Considering the cost of data sampling using WEST simula-
225 tions, yet in the real world, curriculum learning could be of
226 great help to stabilize the entire procedure, and reduce con-
227 vergence time by several orders of magnitude. Furthermore,
228 each new experimental campaign on WEST requires the def-
229 inition of multiple control scenarios. The latter might have
230 shared plasma states, and overall control objectives. This
231 means that the same events can be used within different sce-
232 narios, especially while choosing initial conditions or termi-
233 nal ones. Since a scenario is a sequence of events, their or-
234 dering already defines a curriculum in an implicit manner,
235 as plasma equilibriums must follow each other in a realistic
236 and feasible way. Moreover, one could go further by explic-
237 itly building a curriculum on the reward function, considering
238 a sequence on its definition, i.e directly on the explicit con-
239 trol objective which might be similar between scenarios. A
240 simple reward on the shape for example could be used as a
241 starter, latter including the elongation, etc. Both ideas lead to
242 the same conclusion regarding CL in fusion:

- 243 • curriculum generation and ordering could describe tasks
244 as events, or intermediate reward definitions;
- 245 • the two approaches shows that a curriculum working for
246 one plasma scenario, could be intuitively generalizable
247 with little effort on similar ones, enhancing production
248 of controllers for several cases during experimental cam-
249 paigns.

250 It is worth noticing that [Tracey *et al.*, 2023] addressed the
251 initial drawbacks of the method described by [Degrave and
252 *et al.*, 2022], i.e. training speed and steady-state performance
253 of the controller. Their approach resembles curriculum learn-
254 ing by borrowing its codes. Researchers partitions a target
255 scenario in smaller chunks, each related to one part of the
256 general task. Distributed environments are then divided into
257 subsets of different cardinalities, each linked to one of the
258 said chunks. Experiences are accumulated from MDPs that
259 differs implicitly in their underlying dynamics. Sampled ex-
260 periences are more diverse, and mix multiple levels of diffi-
261 culty inside the same training procedure. This procedure al-
262 ready reduced training time by a factor of 4. However, despite
263 different initial state distributions, the overall task remain the
264 same between chunks, and no proper curriculum is defined,
265 i.e no knowledge transfer is present and task ordering is not
266 specifically mentioned.

3.2 Curriculum definition

Formalism Let τ be a set of tasks with $m_i : (\mathcal{S}, \mathcal{A}, P_i, R_i) \in \tau$, all sharing the same state and action space. Moreover, we denote \mathcal{D}^τ , the set of all transitions belonging to τ , so that $\mathcal{D}^\tau = \{(s, a, r, s') \mid \exists m_i \in \tau, s \in \mathcal{S}, a \in \mathcal{A}, s' \sim P_i(\cdot|s, a), r = R_i(s, a)\}$. A curriculum \mathcal{C} can then be defined as a direct acyclic graph $(\mathcal{V}, \varepsilon, H, \tau)$, with \mathcal{V} vertices, ε edges, $H : \mathcal{V} \rightarrow \mathcal{P}(\mathcal{D}^\tau)$, connecting $v \in \mathcal{V}$ to a subset of samples of \mathcal{D}^τ . An edge $\langle v_j, v_k \rangle$ of \mathcal{C} links two tasks, using all samples associated by H to v_j before transferring to v_k . For each $m_i \in \tau$, we have $\mathcal{D}_i^\tau = \{(s, a, r, s') \mid s \in \mathcal{S}_i = \mathcal{S}, a \in \mathcal{A}_i = \mathcal{A}, s' \sim P_i(\cdot|s, a), r = R_i(s, a)\}$. We need to associate all $v \in \mathcal{V}$ with corresponding m_i and \mathcal{D}_i^τ , meaning that each path on the graph directly influences how $H : \mathcal{V} \rightarrow \{\mathcal{D}_i^\tau \mid m_i \in \tau\}$ filter knowledge transfer between tasks, with edges built on properties of the samples associated with successive nodes. Indeed, tasks must be ordered properly so that π_i^* is useful for acquiring good samples at each transition to the current vertex. In our case, a task is associated with only one vertex, and each intermediate vertex sinks in only one node until the final one is reached, i.e the final task [Narvekar *et al.*, 2020]. This defines an oriented sequence of tasks, similar to what was previously stated in terms of curriculum learning.

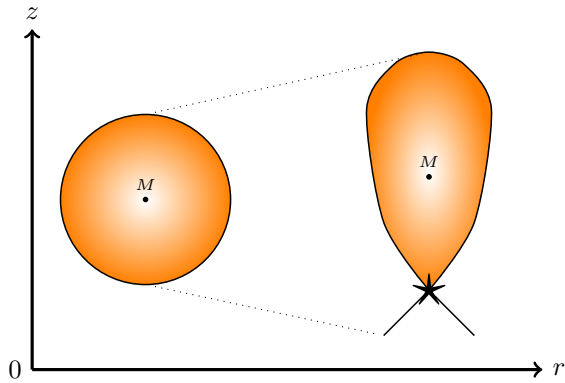


Figure 3: Schematic view of the scenario of interest. It starts from a limiter configuration, and ends up by stabilizing an elongated plasma in an x-point configuration.

Tasks In this work, we consider only one of the two possibilities mentioned earlier. Indeed, tasks are defined on the reward function, and only one scenario is considered for learning a controller. We focus on transitioning from a "circular" shaped plasma in limiter configuration, to an elongated plasma in X-point configuration, i.e $\kappa > 1$ (Figure 3). Elongated configurations have improved thermal confinement properties compared to limiter plasmas, at the cost of developing growing vertical instabilities which make control more difficult. Once formed, the *Last Closed Flux Surface* (LCFS) defines the plasma boundary and the X-point appears at its intersection. The chosen curriculum is entirely conditioned by a set of predefined rewards R_i . This means that while it could have been defined automatically, the uncertainty around tokamak dynamics makes the choice for a handcrafted sequence of tasks quite straightforward for this first application.

Prior control experience on the device informs on which tasks could be considered easier than others. This work then relies on human experts for both determining τ , as well as the resulting sequence order based on \mathcal{V} and ε . More precisely, the curriculum has been built from physical intuition around several key control challenges studied for all tokamaks (Figure 4):

- vertical stabilization of elongated plasmas while tracking plasma current is a well-known control problem. Using classical feedback control, simple proportional-integral-derivative (PID) controllers [Ang *et al.*, 2005] can stabilize plasma's magnetic center (m_r, m_z) , as well as plasma current I_p . Their relative simplicity are not far from a basic RL-based solution, as a naive agent can be summarized as proportional-integral control which reduces errors between measurements and targets. The initial reward function then includes targets for the two elements of interest. Hence, handling such classical problem is a good start in order to build strong foundations for the next tasks;
- tracking the entire plasma boundary becomes more challenging, as approaches from classical control often relies on more advanced methods to synthesize efficient controllers. Since the difficulty becomes more important, we add the LCFS as well as the elongation to the initial targets. This creates a way to guide the agent towards an elongated shape, properly positioning it before the final task;
- finally, once the plasma is set up towards its X-point configuration, we modify the reward to include targets on the X-point itself (distance, magnetic flux, etc). This could be considered as a fine-tuning exploration, since the agent must have already positioned the plasma boundary according to the final configuration. Nevertheless, we must proceed with caution, in order to avoid losing accuracy on previous tasks through catastrophic forgetting [Goodfellow *et al.*, 2015].

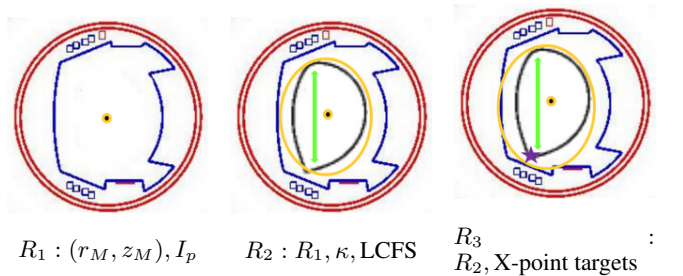


Figure 4: Curriculum overview. We start from a simple vertical control stabilization problem with a free plasma current, to a complex one involving shape and X point.

Transfer learning We transfer the policy and the action-value function between tasks, as both of them are neural networks. The parameters of Q_i learned during an intermediate task, serves as initialization for the parameters of the

348 next action-value function Q_j , without any freezing procedure
 349 which could negatively impact transfer [Wotczyk *et al.*,
 350 2022]. Doing so bias the agent towards more efficient exploration
 351 in the next domain. The policy’s weights are also used
 352 to initialize the parameters of the new one, again without
 353 any freezing procedure. One could have incrementally
 354 frozen layers between tasks in order to keep previous representations
 355 learned by the controller. However, we empirically observed
 356 that it is not necessary for the curriculum learning to work
 357 well in practice. Furthermore, it limits the amount of tasks
 358 present in the curriculum, as the number of layers is bounded.
 359 We further use *potential-based advice* reward shaping (PBARS)
 360 so that $R'_j(s, a) = R_i(s, a) + F(s, a) + R_j(s, a)$
 361 with $F(s, a, s', a') = Q_i(s', a') - Q_i(s, a)$. R_i retains
 362 knowledge from the source task and F encourages exploration
 363 from states that were valuable and overlap with the target j .
 364 They form the potential-based bonus with guarantees that it will
 365 not change the optimal policy [Harutyunyan *et al.*, 2015].

366 **Transfer metrics** While final performance on the target
 367 task will be analyzed, our main objective is to observe how
 368 CL could produce RL-based magnetic controllers faster, for
 369 routine use on WEST. Metrics must be chosen accordingly in
 370 order to measure by how much it speeds up training, compared
 371 to the vanilla method where the agent learn directly on the
 372 final task. We will refer to this question with two tools:
 373 the *jumpstart* and the *Time to threshold* (TTT). The former
 374 measures the initial performance increase at the beginning of
 375 each new task either for a unique task, or as a result of transfer;
 376 the latter checks how much faster the agent learns the policy
 377 which achieves a threshold on the episode return, with or
 378 without curriculum. Each intermediate task is capped to a
 379 maximum duration of 60 episodes, mostly to stay in line with
 380 empirical observations regarding MPO’s warmup phase, i.e
 381 the phase during which NN do not undergo real variations.

382 4 Experiments

383 4.1 Setup

384 **The NICE code** The environment is based on the NICE
 385 C++ code [Faugeras, 2020], which solves the *Grad-Shafranov*
 386 equation [Wesson, 2004] for the plasma domain, with resistive
 387 diffusion [Heumann, 2021] and transport equation enabled.
 388 We use its forward evolution mode which computes the environment’s
 389 state at each timestep. Moreover, power supply and diagnostic
 390 models are implemented in order to account for bias, delays and
 391 offsets of actuators. Overall, it gives an accurate representation
 392 of the plasma, as well as the WEST control system. NICE is
 393 safely initialized to a limiter shaped plasma extracted from
 394 recent experimental data, and whose internal profiles are
 395 randomized to promote diversity among examples. The relative
 396 error of the Newton solver is increased to accelerate execution
 397 without significant loose of accuracy in its outputs. Termination
 398 is triggered if thresholds are reached on active coils currents
 399 or safety factor (proportional to the geometry of the plasma
 400 and its current), to avoid any damage on the device. Episodes
 401 typically last for 500ms, as it appeared enough for generalization
 402 on longer shots.
 403

State and Action spaces The environment’s state is defined
 404 as $s = \{y, I_a, m\}$ with y the plasma equilibrium information,
 405 I_a the currents in the active control coils, and m the raw
 406 magnetic measurements. y typically contains all quantities of
 407 interest described in the curriculum definition. It is usually
 408 difficult to observe the entirety of s in real-time. To overcome
 409 this issue, the learned policy is restricted to a *Partially
 410 Observable MDP* (POMDP) where the state space is limited to
 411 the observation space \mathcal{O} . As such, we have $o(s) = \{tr, m_b, fl, I_a, \frac{dm_b}{dt}\}$,
 412 with tr target references, $\{m_b, fl\}$ magnetic probes and flux
 413 loops raw measurements, and $\frac{dm_b}{dt}$, temporal derivatives of
 414 magnetic probes signals. Noise is injected in observations at
 415 each timestep from Gaussian laws with parameters identified
 416 from WEST plasma discharges database, as well as delays to
 417 model real data acquisition from sensors. For actions, voltages
 418 are sampled from Gaussian distributions which parameters are
 419 the outputs of the control policy, and then supplied to each
 420 of the 11 PFCs circumventing the device (Figure 1 - Naming
 421 conventions stated in Figure 2). After exploring possible
 422 outcomes during training, only the mean of each distribution
 423 is kept at inference to predict optimal actions. Offsets, bias
 424 and delays are part of the power supply model within NICE
 425 to ensure correct handling of WEST actuators in the real world.
 426
 427

Component	Good	Bad	α	weight
LCFS [m]	0.005	0.1	-1	3.
Magnetic center [m]	0.002	0.03	x	1.
κ	0.005	0.03	x	1.
I_p [kA]	0.5	20	x	3.
X point distance [m]	0.01	0.15	x	2.
Flux at current x point	0.	1.	x	2.
Flux at target x point	0.	0.08	x	2.
Flux gradient at target x point	0.	4.	x	1.
Final combiner: <i>Smoothmax</i> ($\alpha = -0.5$)				

Table 1: Reward components description with dimensions. Scaling to $[0, 1]$ range is performed, before combination to a final scalar value. Alpha is specified for each component if it has multiple targets. Flux setpoints are set to 1 since their measure is normalized, while flux gradient must tend towards zero.

Rewards Each reward R_i is a normalized weighted combination
 428 of error signals, extended with PBARS. Each component c_i^j
 429 is computed as the difference E_j between its target value
 430 and the one retrieved from the environment, then scaled to
 431 $[0, 1]$ with *Softplus*(E_j) := $\min(\max(2 \cdot \sigma(-\xi(\frac{E_j - \text{good}}{\text{bad} - \text{good}})), 0), 1)$. They are then
 432 combined into a final scalar within the same interval using the
 433 function *Smoothmax*(α, R_i, W) := $\sum_j w_j R_i^j e^{\alpha R_i^j} / \sum_j w_j e^{\alpha R_i^j}$. If one
 434 component is made out of several targets, an intermediate
 435 combination using the latter is also performed. *Good* and
 436 *bad* parameters in the *Softplus* formulation, scales the reward
 437 signal according to regions of interest in the reward space.
 438 Tight values in both parameters will lead to higher focus on
 439 the component to achieve high reward. Smoother values will
 440 help exploration at the cost of precise control. Weights in the
 441 *Smoothmax* definition affects the importance of each reward
 442
 443

444 component, while the α defines focus balance between them.
 445 Specifically, we combine all 32 distances of the LCFS with
 446 $w = 1$ and $\alpha = -1$. Reward undergo a final scaling, so
 447 that the maximum cumulative reward for 500 ms equals 50.
 448 For a description of each component’s weight and parameters,
 449 please refer to table 1.

450 **Agent** In this work, a distributed *Maximum à Posteriori*
 451 *Policy Optimization* (MPO) [Abdolmaleki and et al., 2018a;
 452 Abdolmaleki and et al., 2018b] is used, which have shown
 453 strong empirical results on a wide range of control prob-
 454 lems, including fusion. It is part of a recent interpretation
 455 of RL as probabilistic inference [Levine, 2018]. Since our
 456 environment is computationally expensive, such paradigm is
 457 useful to enhance sample-efficiency and reach faster con-
 458 vergence compared to a variety of policy gradient methods,
 459 while avoiding the use of on-policy algorithm such as *Proxi-*
 460 *mal Policy Optimization* (PPO) [Schulman and et al., 2017].
 461 Our implementation is composed of 95 multi-layered percep-
 462 trons for the actors and a LSTM for the critic. Specifically,
 463 we use stochastic policies which predict a mean and a stan-
 464 dard deviation for each of the 11 control coils. Once training
 465 is completed, exploring possible outcomes is not needed any-
 466 more. As a consequence, only the mean of each distribution is
 467 kept at inference to predict optimal actions. Sequences were
 468 partitioned so that a *burn-in* phase would take place at each
 469 learner step, i.e. part of each input sequence sampled from
 470 the replay buffer is used to initialize the LSTM core [Kaptur-
 471 owski and et al., 2018]. Adam optimizer was used both in the
 472 critic and the actor networks. Specific hyperparameters cho-
 473 sen for NNs definition can be found in table 2, with others as
 474 well as initialization practices following [Kerboua-Benlarbi
 475 et al., 2024].

Hyperparameter	Chosen value
Batch size	256
Discount factor	0.99
Sequence length for critic	64
Burn-in length critic	10
π_σ	0.5
ϵ	0.5
ϵ_μ	9.09e-5
ϵ_σ	9.09e-8
learning rate	3e-4
dual learning rate	1.5e-2

Table 2: Agent’s hyperparameters.

476 **Training framework** The interaction loop can be described
 477 as follows: a learner worker uses information gathered within
 478 a replay buffer to optimize policy and critic NNs; actor
 479 threads work independently from each other. Each thread
 480 spans a UDS protocol client-server interface with its own ran-
 481 dom seed, in which the policy interacts with an instance of
 482 NICE, sending data to the replay buffer asynchronously; each
 483 actor updates its control policy by copying weights periodi-
 484 cally from the learner. Evaluation is performed on a sepa-
 485 rate thread during training using only the mean of the current
 486 policy as stated before. This results in a fast and reliable,

multi-language, multi-threaded and multi-GPU framework,
 running numerous instances of the NICE environment in par-
 allel to learn a control policy in Python (Figure 5). Policy
 networks were all restricted to CPU, in order to lower sim-
 ulation to reality gaps. Every aspect of the framework then
 ensures that training can put the agent in realistic conditions
 with regards to the machine’s usual operation. Experiments
 are performed on a NVIDIA[®] Tesla[™] V100S for the learner,
 and Intel[®] Cascade Lake[®] 6248 at 2.50GHz for the C++ en-
 vironments. As a side note, the framework is flexible enough
 to allow fast update or addition of new control scenarios.

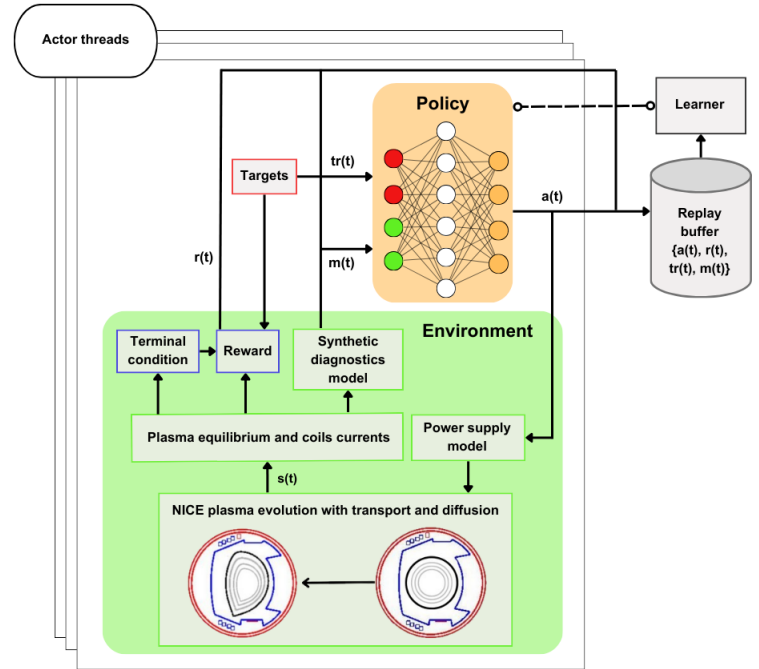


Figure 5: Framework’s overview.

4.2 Results

Training results are averaged over 3 different seeds of the
 evaluator thread. The reward threshold for the TTT is set to
 20, as control starts to perform well in such conditions.

Firstly, we know that an environment’s step within NICE
 lasts for about 13 seconds on average during exploration,
 since the plasma reaches locations of the vacuum chamber in
 which convergence of the simulation is more difficult. This
 means that in the complex case, where poor reward signals are
 common, exploration is long and tedious, increasing comput-
 ing time of an episode up to 2 hours. Based on this idea, the
 monitored training time for the vanilla method easily reaches
 the symbolic threshold of an entire week. Moreover, the re-
 ward never exceeds 10 in average, even with training outside
 the 60 episodes cap scope, which is way under our expecta-
 tions regarding TTT (Figure 7 - upper). One could mention
 the fact that we could have undergo further hyperparameters
 search on the reward definition. However, we kept it general
 enough to avoid overspecializing the method towards one sce-
 nario, leaving more room for adaptation. On the other hand,

518 the CL procedure implicitly leads to reachable states that are
 519 easier at the beginning of the initial task. As a consequence,
 520 the duration of a simulation’s step in this case is shorter in
 521 average, and the simulation converges to an equilibrium in
 522 about 2 seconds. Next tasks follow on top of this idea, which
 523 leads to 10 seconds in average for what is remaining from the
 524 curriculum. This leads to episodes computed at worst in 1
 525 hour for complex tasks, which is already an interesting out-
 526 come. With that in mind, the reward threshold is reached in
 527 about 100 episodes, and the TTT is reduced to approximately
 528 60 hours. As a matter of fact, we observe a clear reduction
 529 in convergence time towards the reward threshold, sufficient
 530 to gain proper control of the plasma in the configuration of
 531 interest (Figure 6a). We stopped training before 60 episodes
 532 for the final task, since the return was stable above 20.

533 If we look at the jumpstart using the total number of
 534 episodes, CL actually performs equally, if not worse, than
 535 the vanilla method for each curriculum steps (Figure 7 - up-
 536 per). A simple explanation comes from the fact that the
 537 added reward complexity inevitably drops the initial return.
 538 Another explanation could arise from so-called catastrophic
 539 forgetting. After those sudden drops, the agent fails its first
 540 attempt, especially on the last task, but ends up recovering.
 541 Recall that we are not stopping previous tasks based on per-
 542 formance, but rather constraining the entire training time to
 543 60 episodes. So, this situation is not entirely surprising, since
 544 no optimal behavior was guaranteed at the end of each in-
 545 termediate curriculum step. Moreover, MPO requires several
 546 initial exploratory episodes, in order for training to start con-
 547 cretely. This means that the overall method could also be
 548 analyzed without those warm-up interactions, restricting the
 549 figure to the last 20 meaningful episodes for example (Figure
 550 7 - lower). In this case, both metrics gives better results, as
 551 only improved behaviors are taken into account: the jump-
 552 start is significantly higher, despite the last drop for the last
 553 transition, and the time to threshold is even lower. Actu-
 554 ally, drooping the warm-up interactions becomes even more
 555 meaningful if we extend transfer to the overall MPO’s inter-
 556 nal mechanism. A such, exploration would not be as strong as
 557 at MPO’s initialization, and fine-tuning would be predominant
 558 throughout the reward function.

559 CL does clearly improve the average performance on the
 560 final task (Figure 6b), as it performs better than the vanilla
 561 policy (Figures 7 - both). It enhances magnetic control, show-
 562 ing that the method does not induce any training instabilities,
 563 apart from potential catastrophic forgetting.

Method	Jumpstart on the final task	TTT
Vanilla	4.3	180h
CL	-10.2	60h

(a) Transfer metrics.

	Episode mean reward	Error margin
Vanilla	5.2	± 3.65
CL	18.4	± 4.23

(b) Mean error for each component.

Figure 6: Analysis of the vanilla control policy against the CL method.

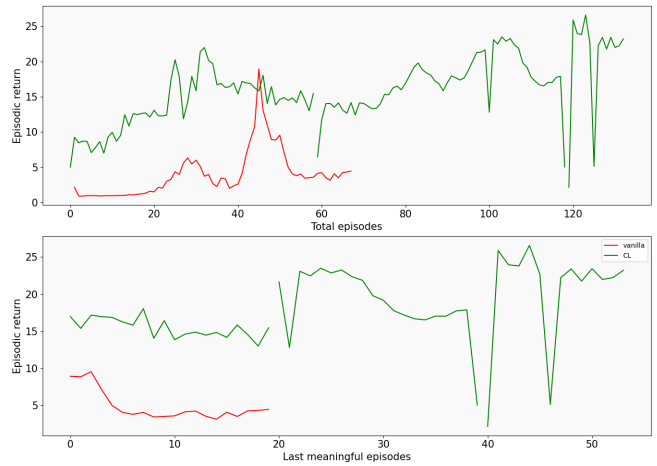


Figure 7: Episodic return for both methods (vanilla - red, CL - green). Since MPO takes several hours to properly start learning, we consider the last episodes that were meaningful regarding reward convergence.

5 Conclusion and perspectives

Curriculum learning displays interesting results in terms of convergence time, while reaching higher levels of performance that a controller exhibits when trained from scratch. Through the simple definition of a sequence of tasks in terms of reward functions, robust magnetic controllers are obtained three times faster than baseline training which requires at least a week.

This work is one of the first attempts along with [Tracey *et al.*, 2023] to look for practical means of speeding up training of RL-based magnetic controllers. The two methods are also not orthogonal, and combining them could lead to training times even shorter. Moreover, we fixed the action space between tasks, but using the 11 coils might not be useful all the time. Same goes for the magnetic measurements, since nothing indicates that all sensors are useful all the time. Automatic sequencing of the action and state spaces definitions could help in improving the curriculum generation.

A clear limitation of the method comes from the risk of catastrophic forgetting, since we transfer without freezing procedure. A perspective lies in the use of *Progressive Neural Networks* (PNN)[Rusu *et al.*, 2016b], which are not affected by catastrophic forgetting and are theoretically capable of handling complete different tasks. However, big architectures can not efficiently work on real-time control systems due to predictions slower than the timescale of many plasma events. One solution could come from *Policy Distillation* [Rusu *et al.*, 2016a]. By training PNNs through curriculum learning, powerful expert policies could be obtained quickly, and distilled into a smaller network in line with our operational constraints.

References

[Abdolmaleki and et al., 2018a] Abbas Abdolmaleki and Jost Tobias Springenberg et al. Maximum a posteriori

- 598 policy optimisation. *arXiv preprint arXiv:1806.06920*,
599 2018.
- 600 [Abdolmaleki and et al., 2018b] Abbas Abdolmaleki and
601 Jost Tobias Springenberg et al. Relative entropy regular-
602 ized policy iteration. *arXiv preprint arXiv:1812.02256*,
603 2018.
- 604 [Ang et al., 2005] Kiam Heong Ang, G. Chong, and Yun Li.
605 Pid control system analysis, design, and technology. *IEEE*
606 *Transactions on Control Systems Technology*, 13(4):559–
607 576, 2005.
- 608 [Ariola and Pironi, 2008] Marco Ariola and Alfredo Pironi.
609 *Magnetic Control of Tokamak Plasmas*. Springer London,
610 2008.
- 611 [Bengio et al., 2009] Yoshua Bengio, Jerome Louradour,
612 Ronan Collobert, and Jason Weston. Curriculum learning.
613 In *Proceedings of the 26th Annual International Confer-*
614 *ence on Machine Learning*, page 41–48. Association for
615 Computing Machinery, 2009.
- 616 [Bourdelle and et al., 2015] Clarisse Bourdelle and Jean-
617 François Artaud et al. West physics basis. *Nuclear Fusion*,
618 55(6):063–017, may 2015.
- 619 [Brohan and et al., 2023] Anthony Brohan and Noah Brown
620 et al. Rt-1: Robotics transformer for real-world control at
621 scale. 2023.
- 622 [Bucalossi and et al., 2022] Jerome Bucalossi and
623 Joelle Achard et al. Operating a full tungsten ac-
624 tively cooled tokamak: overview of west first phase of
625 operation. *Nuclear Fusion*, 62(4):042007, feb 2022.
- 626 [Carpanese, 2021] Francesco Carpanese. Development of
627 free-boundary equilibrium and transport solvers for sim-
628 ulation and real-time interpretation of tokamak experi-
629 ments. page 238, 2021.
- 630 [Char and et al., 2023] Ian Char and Joseph Abbate et al.
631 Offline model-based reinforcement learning for tokamak
632 control. volume 211 of *Proceedings of Machine Learning*
633 *Research*, pages 1357–1372. PMLR, 15–16 Jun 2023.
- 634 [De Tommasi et al., 2022] Gianmaria De Tommasi, Sara
635 Dubbioso, and Yao Huang et al. A rl-based vertical sta-
636 bilization system for the east tokamak. In *2022 American*
637 *Control Conference (ACC)*, pages 5328–5333, 2022.
- 638 [Degrave and et al., 2022] Jonas Degrave and Federico Fe-
639 licci et al. Magnetic control of tokamak plasmas through
640 deep reinforcement learning. *Nature*, 602(7897):414–419,
641 2022.
- 642 [Dubbioso et al., 2023] Sara Dubbioso, Gianmaria De Tom-
643 masi, and Adriano Mele et al. A deep reinforcement learn-
644 ing approach for vertical stabilization of tokamak plasmas.
645 *Fusion Engineering and Design*, 194:113725, 2023.
- 646 [Faugeras, 2020] Blaise Faugeras. An overview of the nu-
647 merical methods for tokamak plasma equilibrium compu-
648 tation implemented in the nice code. *Fusion Engineering*
649 *and Design*, 160:112020, 2020.
- 650 [Fujimoto et al., 2018] Scott Fujimoto, Herke Hoof, and
651 David Meger. Addressing function approximation error in
actor-critic methods. In *International conference on ma-*
chine learning, pages 1587–1596. PMLR, 2018.
- [Goodfellow et al., 2015] Ian J. Goodfellow, Mehdi Mirza,
Da Xiao, Aaron Courville, and Yoshua Bengio. An em-
pirical investigation of catastrophic forgetting in gradient-
based neural networks, 2015.
- [Graves et al., 2017] Alex Graves, Marc G. Bellemare, Jacob
Menick, Remi Munos, and Koray Kavukcuoglu. Auto-
mated curriculum learning for neural networks, 2017.
- [Grondman et al., 2012] Ivo Grondman, Lucian Busoniu,
Gabriel A. D. Lopes, and Robert Babuska. A survey
of actor-critic reinforcement learning: Standard and nat-
ural policy gradients. *IEEE Transactions on Systems,*
Man, and Cybernetics, Part C (Applications and Reviews),
42(6):1291–1307, 2012.
- [Haarnoja et al., 2018] Tuomas Haarnoja, Aurick Zhou,
Pieter Abbeel, and Sergey Levine. Soft actor-critic:
Off-policy maximum entropy deep reinforcement learning
with a stochastic actor. In *International conference on ma-*
chine learning, pages 1861–1870. PMLR, 2018.
- [Han et al., 2023] Dong Han, Beni Mulyana, Vladimir
Stankovic, and Samuel Cheng. A survey on deep rein-
forcement learning algorithms for robotic manipulation.
Sensors, 23(7), 2023.
- [Harutyunyan et al., 2015] Anna Harutyunyan, Sam Devlin,
Peter Vrancx, and Ann Nowe. Expressing arbitrary re-
ward functions as potential-based advice. *Proceedings of*
the AAAI Conference on Artificial Intelligence, 29(1), Feb.
2015.
- [Heumann, 2021] H. Heumann. A galerkin method for the
weak formulation of current diffusion and force balance in
tokamak plasmas. *Journal of Computational Physics*, 442,
2021.
- [Ivanovic and et al., 2019] Boris Ivanovic and James Harri-
son et al. Barc: Backward reachability curriculum for
robotic reinforcement learning. In *2019 International*
Conference on Robotics and Automation (ICRA), pages
15–21. IEEE, 2019.
- [Kapturowski and et al., 2018] Steven Kapturowski and
Georg Ostrovski et al. Recurrent experience replay
in distributed reinforcement learning. In *International*
Conference on Learning Representations, 2018.
- [Kerboua-Benlarbi et al., 2024] S. Kerboua-Benlarbi,
R. Nouailletas, B. Faugeras, E. Nardon, and P. Moreau.
Magnetic control of west plasmas through deep reinforc-
ement learning. *IEEE Transactions on Plasma Science*,
pages 1–0, 2024.
- [Kiran and et al., 2022] B. Ravi Kiran and Ibrahim Sobh
et al. Deep reinforcement learning for autonomous driv-
ing: A survey. *IEEE Transactions on Intelligent Trans-*
portation Systems, 23(6):4909–4926, 2022.
- [Levine, 2018] Sergey Levine. Reinforcement learning and
control as probabilistic inference: Tutorial and review,
2018.

- 706 [Lillicrap and et al., 2015] Timothy P. Lillicrap and Jonathan
707 J. Hunt et al. Continuous control with deep reinforcement
708 learning. *arXiv preprint arXiv:1509.02971*, 2015.
- 709 [MacAlpine and Stone, 2018] Patrick MacAlpine and Peter
710 Stone. Overlapping layered learning. *Artificial Intelli-*
711 *gence*, 254:21–43, 2018.
- 712 [Meade, 2009] Dale Meade. 50 years of fusion research. *Nu-*
713 *clear Fusion*, 50(1):014004, dec 2009.
- 714 [Mnih and et al., 2016] Volodymyr Mnih and Adria Puig-
715 domenech Badia et al. Asynchronous methods for deep re-
716 inforcement learning. In *International conference on ma-*
717 *chine learning*, pages 1928–1937. PMLR, 2016.
- 718 [Narvekar et al., 2020] Sanmit Narvekar, Bei Peng, and Mat-
719 teo Leonetti et al. Curriculum learning for reinforcement
720 learning domains: A framework and survey. *The Journal*
721 *of Machine Learning Research*, 21(1):7382–7431, 2020.
- 722 [Nouailletas and et al., 2023] Rémy Nouailletas and
723 Philippe Moreau et al. West plasma control system
724 status. *Fusion Engineering and Design*, 192:113582,
725 2023.
- 726 [Rusu et al., 2016a] Andrei A. Rusu, Sergio Gomez Col-
727 menarejo, Caglar Gulcehre, Guillaume Desjardins, James
728 Kirkpatrick, Razvan Pascanu, Volodymyr Mnih, Koray
729 Kavukcuoglu, and Raia Hadsell. Policy distillation, 2016.
- 730 [Rusu et al., 2016b] Andrei A. Rusu, Neil C. Rabinowitz,
731 Guillaume Desjardins, Hubert Soyer, James Kirkpatrick,
732 Koray Kavukcuoglu, Razvan Pascanu, and Raia Had-
733 sell. Progressive neural networks. *CoRR*, abs/1606.04671,
734 2016.
- 735 [Schulman and et al., 2015] John Schulman and
736 Sergey Levine et al. Trust region policy optimiza-
737 tion. In *International conference on machine learning*,
738 pages 1889–1897. PMLR, 2015.
- 739 [Schulman and et al., 2017] John Schulman and Filip Wol-
740 ski et al. Proximal policy optimization algorithms. *arXiv*
741 *preprint arXiv:1707.06347*, 2017.
- 742 [Seo and et al., 2021] Jaemin Seo and Yong-Su Na et al.
743 Feedforward beta control in the KSTAR tokamak by deep
744 reinforcement learning. *Nuclear Fusion*, 61(10):106010,
745 2021.
- 746 [Seo et al., 2024] Jaemin Seo, SangKyeun Kim, Azarakhsh
747 Jalalvand, Rory Conlin, Andrew Rothstein, Joseph Ab-
748 bate, Keith Erickson, Josiah Wai, Ricardo Shousha, and
749 Egemen Kolemen. Avoiding fusion plasma tearing insta-
750 bility with deep reinforcement learning. *Nature*, 626:746–
751 751, 02 2024.
- 752 [Soviany et al., 2022] Petru Soviany, Radu Tudor Ionescu,
753 Paolo Rota, and Nicu Sebe. Curriculum learning:
754 A survey. *International Journal of Computer Vision*,
755 130(6):1526–1565, 2022.
- 756 [Stanley et al., 2005] Kenneth O. Stanley, Bobby D. Bryant,
757 and Risto Miikkulainen. Evolving neural network agents
758 in the nero video game. 2005.
- [Sutton and Barto, 2018] Richard S. Sutton and Andrew G. 759
Barto. *Reinforcement learning: An introduction*. MIT 760
press, 2018. 761
- [Tracey et al., 2023] Brendan D. Tracey, Andrea Michi et al., 762
and The TCV Team. Towards practical reinforce- 763
ment learning for tokamak magnetic control. *ArXiv*, 764
abs/2307.11546, 2023. 765
- [Wakatsuki and et al., 2019] Takuma Wakatsuki and 766
T. Suzuki et al. Safety factor profile control with re- 767
duced central solenoid flux consumption during plasma 768
current ramp-up phase using a reinforcement learning 769
technique. *Nuclear Fusion*, 59(6):066022, 2019. 770
- [Wakatsuki et al., 2021] Takuma Wakatsuki, T. Suzuki, 771
N. Oyama, and N. Hayashi. Ion temperature gradient con- 772
trol using reinforcement learning technique. *Nuclear Fu-* 773
sion, 61(4):046036, mar 2021. 774
- [Wesson, 2004] John Wesson. Tokamaks 3rd edition. *Jour-* 775
nal of Plasma Physics, 71(3):377–377, 2004. 776
- [Wołczyk et al., 2022] Maciej Wołczyk, Michał Zajac, Raz- 777
van Pascanu, Łukasz Kuciński, and Piotr Miłoś. Disentan- 778
gling transfer in continual reinforcement learning, 2022. 779
- [Wu and Tian, 2017] Yuxin Wu and Yuandong Tian. Train- 780
ing agent for first-person shooter game with actor-critic 781
curriculum learning. In *International Conference on* 782
Learning Representations, 2017. 783
- [Zhu et al., 2023] Zhuangdi Zhu, Kaixiang Lin, Anil K. Jain, 784
and Jiayu Zhou. Transfer learning in deep reinforcement 785
learning: A survey. *IEEE Transactions on Pattern Analysis* 786
and Machine Intelligence, 45(11):13344–13362, 2023. 787